

Cardiac Stem Cells Possess Growth Factor-Receptor Systems That After Activation Regenerate the Infarcted Myocardium, Improving Ventricular Function and Long-Term Survival

Konrad Urbanek,* Marcello Rota,* Stefano Cascapera, Claudia Bearzi, Angelo Nascimbene, Antonella De Angelis, Toru Hosoda, Stefano Chimenti, Mathue Baker, Federica Limana, Daria Nurzynska, Daniele Torella, Francesco Rotatori, Raffaella Rastaldo, Ezio Musso, Federico Quaini, Annarosa Leri, Jan Kajstura, Piero Anversa

Abstract—Cardiac stem cells and early committed cells (CSCs-ECCs) express c-Met and insulin-like growth factor-1 (IGF-1) receptors and synthesize and secrete the corresponding ligands, hepatocyte growth factor (HGF) and IGF-1. HGF mobilizes CSCs-ECCs and IGF-1 promotes their survival and proliferation. Therefore, HGF and IGF-1 were injected in the hearts of infarcted mice to favor, respectively, the translocation of CSCs-ECCs from the surrounding myocardium to the dead tissue and the viability and growth of these cells within the damaged area. To facilitate migration and homing of CSCs-ECCs to the infarct, a growth factor gradient was introduced between the site of storage of primitive cells in the atria and the region bordering the infarct. The newly-formed myocardium contained arterioles, capillaries, and functionally competent myocytes that with time increased in size, improving ventricular performance at healing and long thereafter. The volume of regenerated myocytes was $2200 \mu\text{m}^3$ at 16 days after treatment and reached $5100 \mu\text{m}^3$ at 4 months. In this interval, nearly 20% of myocytes reached the adult phenotype, varying in size from 10 000 to 20 000 μm^3 . Moreover, there were 43 ± 13 arterioles and 155 ± 48 capillaries/ mm^2 myocardium at 16 days, and 31 ± 6 arterioles and 390 ± 56 capillaries at 4 months. Myocardial regeneration induced increased survival and rescued animals with infarcts that were up to 86% of the ventricle, which are commonly fatal. In conclusion, the heart has an endogenous reserve of CSCs-ECCs that can be activated to reconstitute dead myocardium and recover cardiac function. (*Circ Res.* 2005;97:663-673.)

Key Words: cardiac progenitor cells ■ myocardial regeneration ■ mortality

Adult cardiac stem cells (CSCs) and early committed cells (ECCs) express the stem cell antigens c-kit, MDR1, and Sca-1.¹⁻⁴ c-kit^{POS} cells are self-renewing, clonogenic, and multipotent and give rise to myocytes, smooth muscle cells (SMCs), and endothelial cells (ECs) in vitro and in vivo.^{1,5} A similar category of CSCs-ECCs has been found in the human heart,^{6,7} suggesting that these undifferentiated cells participate in the normal turnover of cardiac cells and, under favorable conditions, have the ability to form myocytes, coronary arterioles, and capillary structures.^{1,5,7} The presence of CSCs-ECCs raises the question of why they fail to respond to ischemic injury with regeneration of myocytes and coronary vessels and restoration of function. CSCs-ECCs distributed within the damaged area may die together with parenchymal cells, however, and SMCs and ECs in coronary vessels prevent myocardial repair. For this reason, we have

explored the possibility that CSCs-ECCs, if properly activated, can translocate to sites of damage, survive the unfavorable environment, multiply, and differentiate, forming functionally competent myocardium.

Hepatocyte growth factor (HGF) stimulates cell migration⁸ by expression of metalloproteinases (MMPs)⁹ that by breaking down the extracellular matrix favor cell locomotion, homing, and tissue reconstitution. The receptor of HGF, c-Met, is expressed in bone marrow progenitor cells, satellite cells, and embryonic myocytes.^{10,11} Insulin-like growth factor-1 (IGF-1) is mitogenic, antiapoptotic, and necessary for neural stem cell growth.¹² IGF-1 promotes myocyte formation and attenuates myocyte death after infarction.¹³ Together, these findings prompted us to determine whether CSCs-ECCs express c-Met and whether HGF stimulates their migration to the infarcted myocardium. If CSCs-ECCs ex-

Original received May 25, 2005; revision received August 11, 2005; accepted August 11, 2005.

From the Cardiovascular Research Institute, Department of Medicine, New York Medical College, Valhalla, NY; and the Tardini-Olivetti Stem Cell Center (E.M., F.Q.), Parma, Italy.

*Both authors contributed equally to this study.

Correspondence to Piero Anversa, MD, Cardiovascular Research Institute, Vosburgh Pavilion, New York Medical College, Valhalla, NY 10595. E-mail piero_anversa@nymc.edu

© 2005 American Heart Association, Inc.

Circulation Research is available at <http://circres.ahajournals.org>

DOI: 10.1161/01.RES.0000183733.53101.11

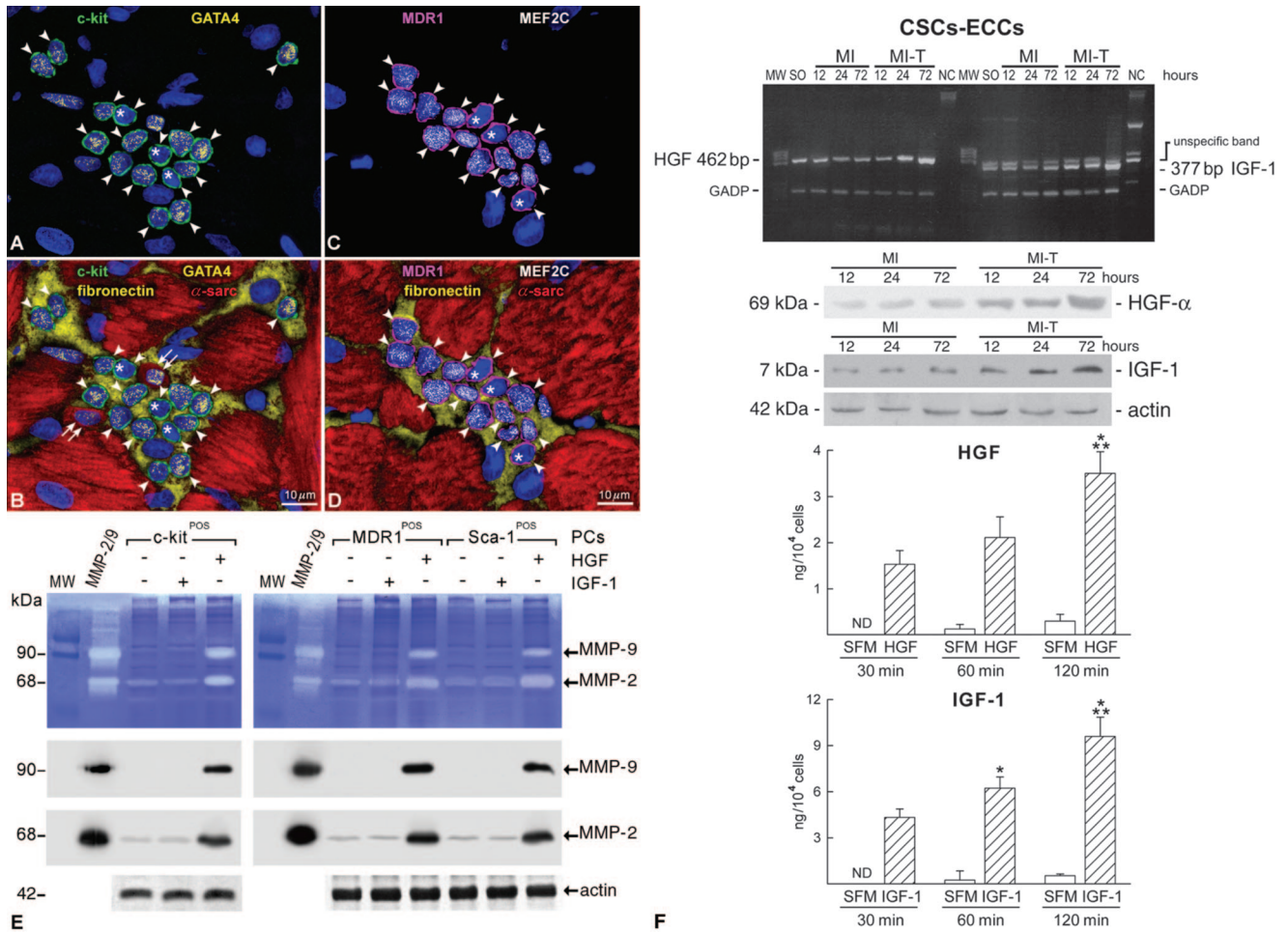


Figure 1. Atrial clusters of CSCs-ECCs. c-kit^{POS} (A and B, green; arrowheads) and MDR1^{POS} (C and D, magenta; arrowheads) cells in normal hearts express GATA-4 (A and B; yellow) and MEF2C (C and D, white) in nuclei. Fibronectin (B and D, yellow) and myocytes (B and D, α -sarcomeric actin; red) are shown. *c-kit^{POS} (A and B) or MDR1^{POS} (C and D) only. Double arrows indicate small-GATA-4^{POS} myocytes (B). E, HGF-IGF-1 and CSCs-ECCs. Gelatinase-activity appears as clear bands against blue background (upper panels). MMP-2 and MMP-9 -protein is also shown (lower-panels). F, HGF and IGF-1 mRNA is enhanced in CSCs-ECCs of GF-treated infarcted hearts. NC indicates negative control. HGF-protein in CSCs-ECCs of GF-treated infarcted hearts increased 3-fold, 3-fold, and 5-fold at 12, 24, and 72 hours, respectively, whereas IGF-1 protein increased 2-fold, 4-fold, and 5-fold. HGF and IGF-1 formed by CSCs-ECCs increased with time (ELISA; lower panels). ND indicates not detectable. * $P < 0.05$, ** $P < 0.01$ versus 30 and 60 minutes.

press IGF-1 receptor, IGF-1 may protect their viability and enhance their growth within the infarct. Thus, myocardial infarction was produced in mice and HGF and/or IGF-1 were locally injected to trigger migration and homing of CSCs-ECCs to the ischemic area. The impact of this intervention on myocardial regeneration, heart function, and animal survival was determined acutely, at healing and long thereafter to evaluate its therapeutic efficacy.

Materials and Methods

Mice were infarcted, treated with IGF-1 and HGF (GFs) and euthanized at different intervals up to 4 months. Myocardial regeneration was determined by confocal microscopy. An expanded Materials and Methods can be found in an online-only data supplement available at <http://circres.ahajournals.org>.

Results

CSCs

CSCs did not express markers of cardiac and hemopoietic cell lineages.¹ They were more numerous in the atria and apex

than in the ventricle (supplemental Figure S1). ECCs expressed transcription factors of cardiac (GATA-4) and myocyte (MEF2C) lineages, identifying progenitor cells (Figure 1A through 1D). Also, c-kit^{POS}, MDR1^{POS}, and Sca-1^{POS} cells expressed α -sarcomeric actin or cardiac myosin, representing myocyte precursors. SMC progenitors and precursors expressed GATA-6 and α -smooth muscle actin and EC progenitors and precursors Ets-1 and von Willebrand factor, respectively (supplemental Figure S2).

c-Met and IGF-1R

Most CSCs-ECCs expressed c-Met and IGF-1 receptor together with HGF and IGF-1 (supplemental Figure S3). Migration studies documented that HGF had a chemoattractive effect on CSCs-ECCs that peaked at 100 ng/mL. Invasion assays showed that 100 ng/mL HGF increased by 7-fold the number of CSCs-ECCs that accumulated in the lower well of a modified Boyden chamber. IGF-1 had few motogenic and invasive properties (supplemental Figure S4). After HGF

administration, CSCs-ECCs had gelatinolytic activity and secreted MMP-2 and MMP-9; IGF-1 had little effects on MMPs (Figure 1E).

IGF-1 and HGF decreased apoptosis of CSCs-ECCs in serum-free medium by 94% and 58%, respectively. Moreover, BrdU^{POS} CSCs-ECCs increased 11-fold with IGF-1 and 3-fold with HGF. The effects of both GFs on cell death and growth were not different from those of IGF-1 alone (supplemental Figure S5). Murine mRNA and protein for IGF-1 and HGF were present in non-stimulated CSCs-ECCs and increased in GF-treated infarcted-hearts (Figure 1H). Animals were injected with heterologous proteins, human IGF-1, and HGF.

HGF and IGF-1 in the supernatant of GF-stimulated CSCs-ECCs in serum-free medium increased from 30 minutes to 120 minutes, reaching a 13-fold and 26-fold elevation at 120 minutes, respectively (Figure 1F). The increase in murine HGF and IGF-1 mRNA, together with the significant accumulation of murine HGF and IGF-1 protein in stimulated CSCs-ECCs *in vivo*, supports the notion that CSCs-ECCs can synthesize these GFs. The time-dependent increase in the secretion of HGF and IGF-1 *in vitro* strengthens this conclusion. Thus, CSCs-ECCs possess the c-Met-HGF and IGF-1 receptor-IGF-1 systems that promote cell growth and migration, attenuate apoptosis, and increase the secretion of their ligands.

Migration of CSCs-ECCs

Because cycling CSCs-ECCs were identified in the atrioventricular (AV) groove (supplemental Figures S6 and S7), a retrovirus expressing enhanced green fluorescence protein (EGFP)¹⁻⁵ was injected in this region to label replicating cells before the administration of the GFs. Integration and accumulation of EGFP in the tagged cells required \approx 48 hours (supplemental Figure S8). Therefore, coronary occlusion was performed 2 days after viral inoculation, and HGF and/or IGF-1 were injected 5 hours later (supplemental Figure S9). Increasing doses of HGF were used between the AV groove and the infarct to favor migration of CSCs-ECCs to the infarct. Fluorescein-conjugated HGF was injected to establish its distribution; fluorescence intensity was higher adjacent to the infarct than in the distant myocardium (Figure 2A through 2C). As shown by ELISA, HGF quantity was also higher in the border than in the remote tissue (Figure 2D). Autocatalytic phosphorylation of c-Met and IGF-1R, phospho-Akt, phospho-IRS-1, and phospho-FAK in c-kit^{POS} CSCs-ECCs showed that these indices of c-Met and IGF-1 receptor activation were barely detectable in untreated hearts. Conversely, their expression in CSCs-ECCs from GF-treated infarcts increased with time (Figure 2E). Phospho-FAK and phospho-c-Met were also detected by immunocytochemistry (data not shown) and fluorescent-activated cell sorter (Figure 2F). Antibody specificity was determined by fluorescent-activated cell sorter, and immunoprecipitation Western blotting of Lewis lung carcinoma cells (Figure 2G and 2H).

The effects of GFs on cell migration were evaluated *ex vivo*. Microscopic fields were analyzed for 1 to 5 hours to measure movement of EGFP^{POS} cells (Figure 3A through 3E). The same EGFP^{POS} cells were then characterized after fixa-

tion: EGFP^{POS} cells expressed antigens typical of CSCs-ECCs (Figure 3F and 3G; supplemental Figure S10). EGFP^{POS} cells, which were not CSCs-ECCs, were occasionally seen in the AV groove; these cells did not move after GF administration. EGFP^{POS} CSCs-ECCs migrated at \approx 70 μ m/h (supplemental Figure S11) from the AV groove to the border and central infarct in 2 to 3 and 6 to 7 hours, respectively. IGF-1 had minimal effect on locomotion. In GF-treated infarcts, the number of EGFP^{POS} CSCs-ECCs and EGFP^{POS}-EGFP^{NEG} CSCs-ECCs in this region increased 3-fold and 8-fold, respectively (supplemental Figure S12). Most CSCs-ECCs expressed both c-Met and IGF-1 receptor and were committed to cardiac lineages (supplemental Figure S13 and S14).

Destiny of CSCs-ECCs

CSCs-ECCs can migrate via the coronary bed, the interstitium, or both. Therefore, the coronary circulation was perfused with rhodamine-labeled dextran, and GFs were administered at the time of observation. The coronary vasculature was recognized by red fluorescence and EGFP^{POS} cells by green fluorescence (Figure 4A through 4D; supplemental Figure S15). In all cases, EGFP^{POS} cells were located outside the vessels, suggesting that the coronary circulation was not implicated in cell migration; EGFP^{POS} cells were found in interstitial tunnels defined by fibronectin (Figure 4E).

The death, survival, and growth of CSCs-ECCs within the infarct was characterized (supplemental Figures S16 through S19) together with the differentiation of EGFP^{POS} CSCs-ECCs in the early stages of myocardial restoration. In the absence of GFs, CSCs-ECCs within the infarct died rapidly, whereas the presence of GFs promoted their survival and replication. Moreover, a time-dependent increase in the number of c-kit^{POS}, MDR1^{POS}, and Sca-1^{POS} cells undergoing the transition from undifferentiated cells to small myocytes was detected. At 1 day, EGFP^{POS} cells expressed stem cell antigens and MEF2C, but sarcomeric proteins were absent. At 2 days, cells were positive for sarcomeric myosin and at 3 to 4 days had developed into small EGFP^{POS} myocytes. Connexin 43 and N-cadherin were present (Figure 5A and 5B). These cells, clustered in patches throughout the infarct, increased with time (Figure 5C). At 1 to 2 days, new arterioles had thick walls and ill-defined lumen. At 3 to 4 days, arterioles and capillaries increased; they were formed by EGFP^{POS} and EGFP^{NEG} cells (supplemental Figure S20).

GFs and Infarct Size

Myocardial infarction rates in GF-treated hearts at 16 days and 4 months were 67% and 63%, respectively. Corresponding values in untreated mice were 42% and 43%. Thus, infarct size was 60% and 47% larger in GF-treated than in untreated mice at the early and late time point, respectively (supplemental Figure S21). This unexpected result was the consequence of a rapid regeneration of dead myocardium induced by GFs, which rescued animals with extremely large infarcts acutely after coronary occlusion. Figure 6A illustrates a 44% infarct, a nearly maximum infarct size compatible with survival in untreated mice at 16 days. The infarct corresponds to a loss of 1.6 million myocytes from a total of 3.6 million. GF-treated mice survived infarcts of 82% (Figure 6B) and

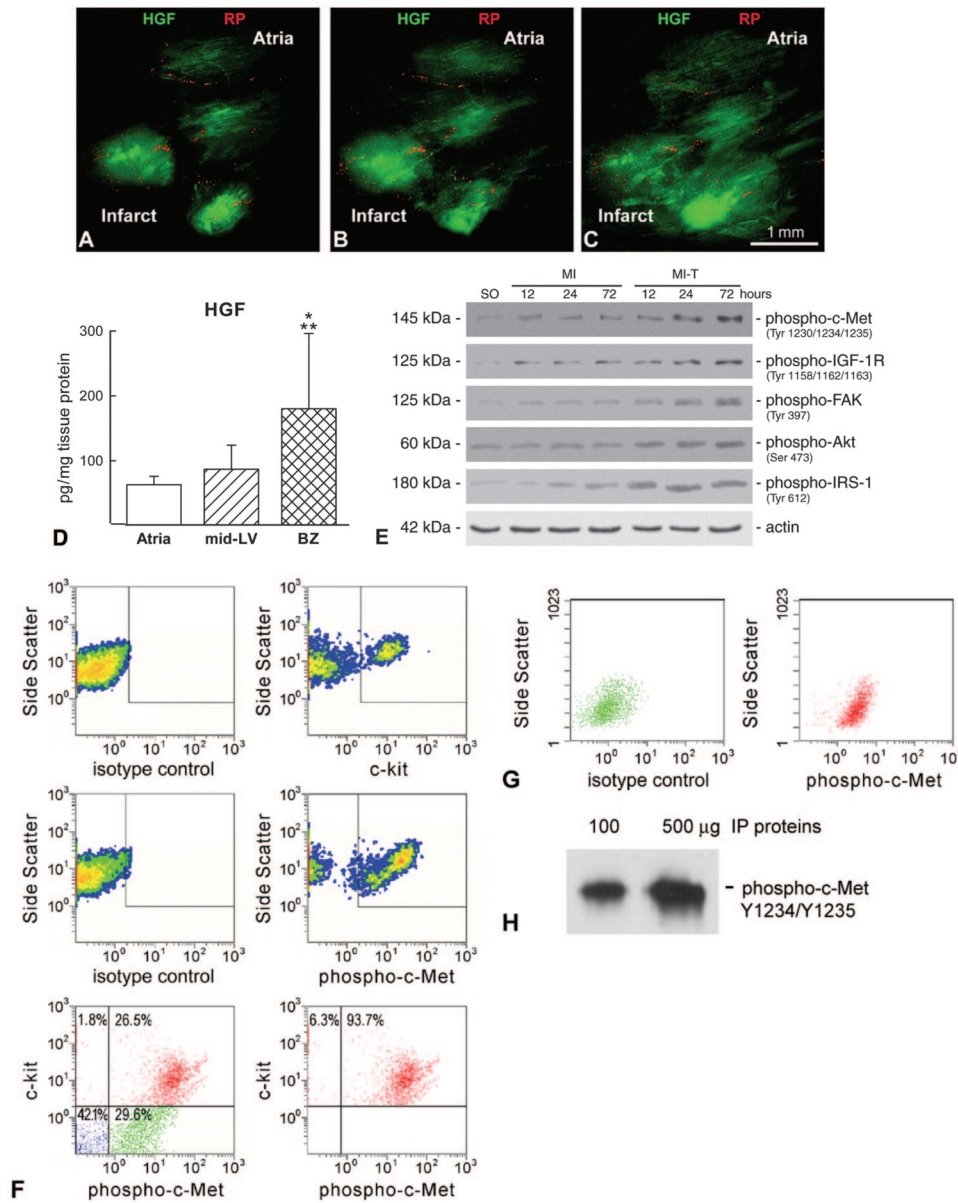


Figure 2. GF administration and CSCs-ECCs. A through C, Fluorescein-labeled HGF is higher at the border zone (BZ) and lower at the AV groove at 10 (A), 30 (B), and 60 (C) minutes after injection. RP indicates rhodamine particles. D, HGF-concentration is higher at BZ, intermediate half-way (mid-LV), and lower at atria. * $P < 0.05$, ** $P < 0.01$ versus BZ and mid-LV. E, Phosphorylated-substrates in CSCs-ECCs of GF-treated infarcted hearts (MI-T) increased ≈ 5 -fold at 12, 24, and 72 hours. F, Density-plots (upper panels) of c-kit^{POS} phospho-c-Met^{POS} cells in MI-T at 24 hours. Dot-plots (lower panels) of c-kit-phospho-c-Met colocalization including c-kit-negative cells (left) and excluding c-kit-negative cells (right). G, Density-plot, Lewis lung carcinoma cells (phospho-c-Met). H, Phospho-c-Met, Lewis lung carcinoma cells.

86%; this is a striking result, as 2.9 and 3.1 million myocytes were lost, respectively.

The group of untreated infarcted mice consisted of 123 animals (supplemental Table S1). The 87 animals that died 10 hours to 15 days after surgery had infarctions of 57% to 82%. Twenty-two of the remaining 36 were euthanized at 16 days, and 15 were studied functionally and structurally. The group of GF-treated infarcted mice consisted of 107 animals. The 46 animals that died 10 hours to 15 days after surgery had infarctions of 63% to 79%. Forty-nine of the remaining 61 were euthanized at 16 days, and 26 were studied. None of untreated mice survived 16 days with infarcts larger than 60%. Conversely, 14 of 22 mice in the GF-treated group survived 16 days with infarcts greater than 60%, and 7 had 75% to 86% infarcts. Of the remaining 14 untreated infarcted mice, 10 survived 4 months and only 1 had an infarct that reached 50%. Of the remaining 12 GF-treated infarcted animals, 10 survived 4 months, and 6 had infarcts greater than

60% (Figure 6C; 68%). Thus, GF-treatment saved mice with infarcts that are typically fatal.

Myocardial Regeneration

Four of 26 GF-treated mice euthanized at 16 days did not respond to GF administration; they were undistinguishable from untreated infarcted mice. Most likely, they were not properly injected with GFs. Similarly, 2 of 10 GF-treated mice at 4 months had no regenerating band. Thus, successful treatment was obtained in 85% and 80% of treated mice. Unsuccessfully treated mice were characterized structurally (supplemental Table S2).

In untreated mice, the infarcts consisted of collagen type I and III (Figure 6A). In treated mice, the regenerated myocardium occupied $65 \pm 8\%$ and $73 \pm 7\%$ of the infarct at 16 days (Figure 6B) and 4 months (Figure 6C), respectively. The new band of myocardium was located in the mid-portion of the wall and, in some cases, replaced the entire wall thickness

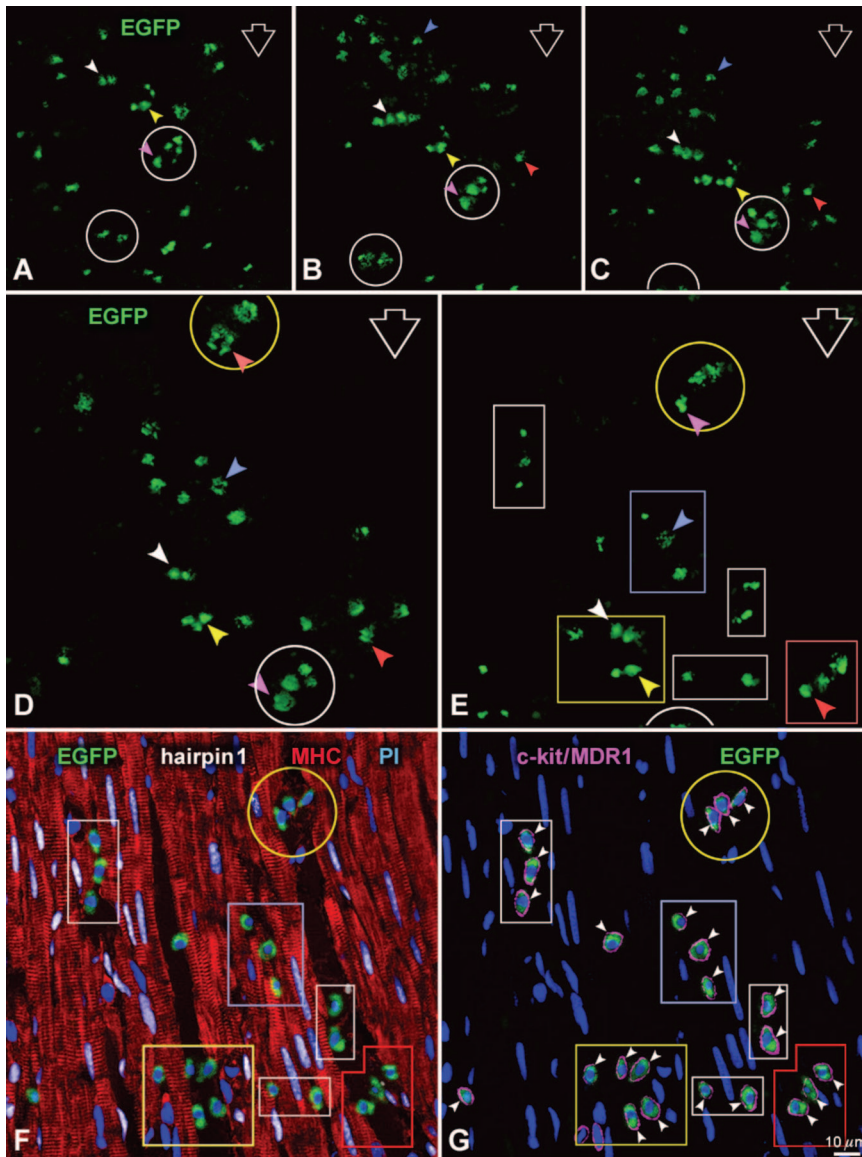


Figure 3. GFs mediate migration of EGFP^{POS} cells. A through E, Heart perfused with Tyrode-solution. Two-photon microscopy images at the BZ 15 hours after infarct and 10 hours after GF administration. Images of the same field were taken 20 minutes apart (A, baseline; B, 20 minutes; C, 40 minutes; D, 60 minutes; E, 80 minutes). EGFP^{POS} cells (green, arrowheads) moved in the direction of large open arrows in 80 minutes. White circles (A) surround EGFP^{POS} cells, which were in the field and then progressively disappeared (C, D, and E). Yellow circle surrounds EGFP^{POS} cells, which appear in D and are in field E. E through G, Rectangles and a yellow circle surround EGFP^{POS} cells detected by 2-photon microscopy (E; green) and confocal microscopy (F; green). Green-fluorescence identifies the same EGFP^{POS} cells (E and F). F, White-fluorescence corresponds to hairpin-1^{POS} apoptotic myocyte-nuclei; EGFP^{POS} cells within the infarct are viable (hairpin-1^{NEG}). Myocytes are cardiac myosin, red. G, EGFP^{POS} cells express c-kit-MDR1 (magenta; arrowheads).

(Figure 6B and 6C). At 16 days, the new myocardium recovered 15% of the infarct, decreasing the infarct size from 67% to 57%. At 4 months, the formed myocardium accounted for 54% of the infarct, reducing infarct size from 63% to 29% (supplemental Figure S22).

The regenerated myocardium was composed of myocytes and coronary vessels. At 16 days, myocytes varied in volume from 600 to 7200 μm^3 and at 4 months, from 700 to 20 000 μm^3 (Figure 6D). At both intervals, treated hearts generated an average 3.2 million myocytes to compensate for a loss of 2.2 million. There were 43 ± 13 arterioles and 155 ± 48 capillaries/ mm^2 at 16 days, and 31 ± 6 arterioles and 390 ± 56 capillaries at 4 months. For comparison, there are ≈ 10 arterioles and ≈ 3500 capillaries/ mm^2 in myocardium in the adult heart. New vessels contained erythrocytes (supplemental Figure S23).

To document that cells in the band were formed after infarction, mice were exposed to BrdU; $84 \pm 9\%$ and $94 \pm 3\%$ myocytes and vessels in the band were BrdU^{POS} at 16 days and 4 months, respectively (Figure 6E and 6F; supplemental Figure S23). At 4 months, the spared myocardium adjacent to and distant from the

infarct had $17 \pm 6\%$ and $8 \pm 3\%$ BrdU^{POS} myocyte nuclei, respectively (supplemental Figure S24). New myocytes were smaller than adult myocytes ($21\,800 \pm 2200 \mu\text{m}^3$) but expressed nestin, desmin, myosin, α -sarcomeric actin, N-cadherin, and connexin 43 (supplemental Figure S25). These results indicate that, in response to HGF and IGF-1, CSCs-ECCs translocate, grow, and differentiate, resulting in significant myocardial regeneration. A single GF had a smaller impact, however, and the 2 GFs acted synergistically in cardiac repair (supplemental Figure S26).

Myocyte Mechanics and Cell Fusion

Myocytes were isolated from regenerated and spared myocardium (Figure 7A through 7F) of GF-treated hearts at 16 days, and their contractile behavior was determined. New cells were smaller than old cells, had BrdU^{POS} nuclei, and resembled neonatal myocytes. Connexin 43 and N-cadherin were detected (Figure 7C through 7F). In comparison with surviving myocytes, new cells exhibited higher peak shortening and velocity of shortening and relengthening (Figure 7G; supplemental Figure S27).

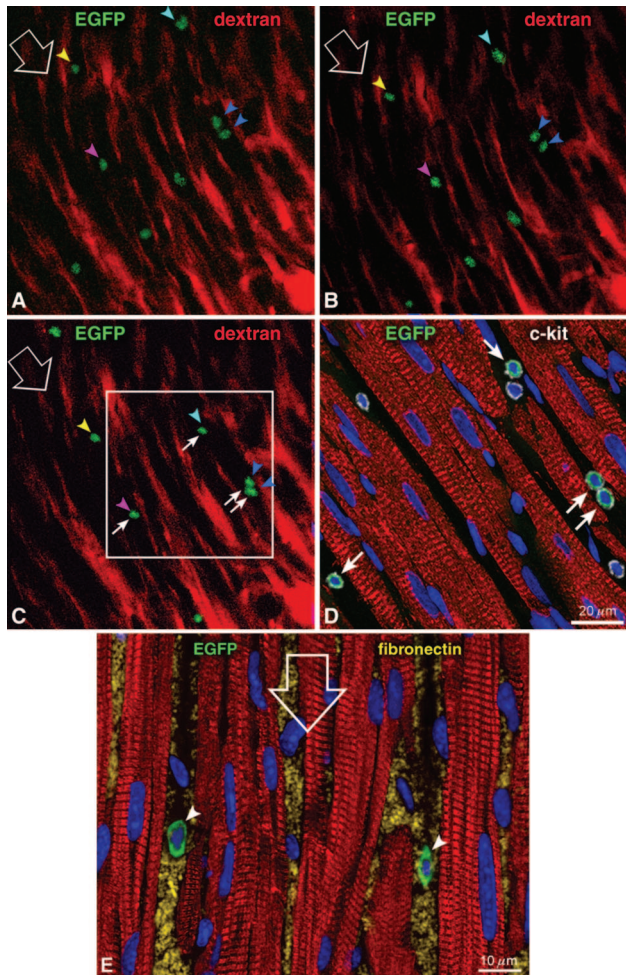


Figure 4. Migration of EGFP^{POS} cells. A through C, Two-photon microscopy images of BZ after perfusion with rhodamine-labeled dextran (red), 5 hours after infarction, and immediately after GF administration. Images were taken 20 minutes apart (A, baseline; B, 20 minutes; C, 40 minutes). EGFP^{POS} cells (green; arrowheads) moved in the direction of large open arrows and in 40 minutes were outside of coronary vessels. D, EGFP^{POS} cells detected by 2-photon microscopy (C, square) and confocal microscopy. Green-fluorescence identifies the same EGFP^{POS} cells (C and D, arrows). D, EGFP^{POS} cells express c-kit (white; arrows). Myocytes indicate cardia -myosin, red. E, EGFP^{POS} cells (arrowheads) within fibronectin-tunnels. Large open arrow indicates the direction of moving cells.

The discrepancy in size between old and new myocytes makes it unlikely that fusion^{1,14} of the activated CSCs with spared myocytes was implicated in the differentiation of these cells into myocytes. Moreover, to rule out fusion of CSCs with other cells, the number of X chromosomes was evaluated in the regenerated myocytes of the female infarcted treated mice. At most, 2 X chromosomes were detected in the nuclei, strongly arguing against cell fusion (Figure 7H). Cycling and noncycling new and old myocytes were identified by Ki67, and DNA content was measured in individual nuclei. Mouse lymphocytes were used as control. Nuclei of noncycling myocytes and lymphocytes had 2C DNA content, whereas Ki67^{POS} nuclei had DNA content intermediately between diploid and tetraploid excluding cell fusion (supplemental Figure S28).

Cardiac Performance and Survival

Contraction in the infarct of GF-treated mice reappeared at 15 days and improved at 1, 3, and 4 -months (Figure 8A through 8E). Hemodynamics improved in GF-treated mice and deteriorated in untreated mice (Figure 8F). In GF-treated hearts, from 16 days to 4 months, left ventricular end-diastolic pressure decreased and LV-developed pressure and dP/dt increased. Also, chamber volume decreased, attenuating diastolic stress (Figure 8F). Together, these variables were responsible for a 34% decrease in animal mortality (Figure 8G), despite \approx 50% larger infarcts in GF-treated animals. Thus, activation of CSCs-ECCs acutely after infarction elicits a sustained regenerative response that ameliorates the anatomy and function of the heart, improving animal survival.

Discussion

The results of the current study demonstrate that the mammalian heart contains a population of resident stem cells and progenitor cells that, after activation, can migrate and invade the infarcted myocardium, leading to a significant reconstitution of the damaged portion of the wall and a remarkable recovery of ventricular function. Myocardial regeneration comprises parenchymal cells and coronary vessels, providing additional evidence in support of the notion that the adult heart possesses an extraordinary growth reserve capable of restoring losses of tissue commonly considered fatal in animals and humans. Commitment of cardiac primitive cells to the myocyte lineage, together with the creation of small actively dividing amplifying myocytes, occurs in the acute phases of cardiac repair, whereas maturation and hypertrophy of the newly formed cells constitute the predominant mechanisms of myocardial regeneration long-term after infarction. Coronary arterioles and capillary structures are produced concurrently with myocytes to ensure adequate oxygenation of the developing myocardium. Differentiation and enlargement of myocytes is paralleled by expansion of the coronary vasculature and microvasculature that tends to preserve blood supply and oxygen diffusion to the surrounding cells. Ultimately, the infarcted heart largely regains its anatomical configuration, dramatically reversing ventricular dilation and thinning of the wall. Although the normal architecture and orientation of myocyte bundles across the wall was not acquired, our findings suggest that local administration of GFs may become a novel powerful therapeutic strategy for the acutely decompensated infarcted heart.

CSCs-ECCs in the Adult Heart

The fact that the heart possesses a stem cell compartment has been shown in several species,^{1-4,15,16} including large animals¹⁷ and humans.^{6,7,18} With one exception,¹⁶ these cells have been characterized by the expression of the typical stem cell antigens c-kit, MDR1 or Sca-1. However, the fact that cardiac primitive cells are self-renewing, clonogenic, and multipotent, which are the critical variables for the definition of a stem cell, has been documented only in rats¹ and dogs.¹⁷ Because of this inevitable premise, it is difficult to reconcile the claim made and terminology used when cells already committed to the myocyte lineage and without established epitopes have been interpreted as a novel class of cardiac

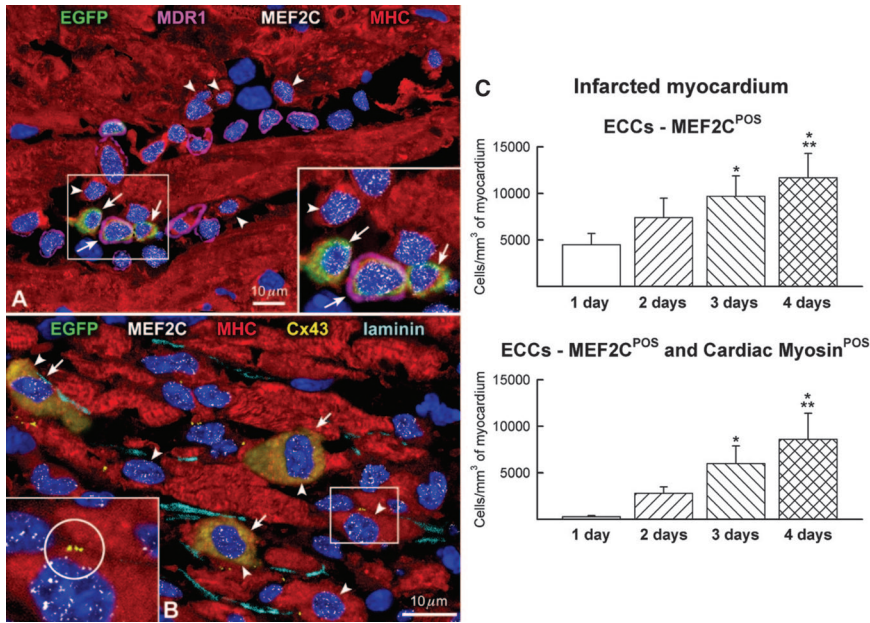


Figure 5. Differentiation of EGFP^{POS} cells. A and B, MI-T at 2 (A) and 4 (B) days. EGFP^{POS} cells (green; arrows), positive (A; magenta) or negative (B) for MDR1 are present within the infarct. Area defined by a rectangle (A and B) is shown at higher magnification in the inset, cells express MEF2C (A and B; white), cardiac myosin (A and B; red), and connexin-43 (B; yellow). Small-myocytes (A and B, arrowheads) are present. In B, laminin appears bright blue. Large myocytes without nuclei reflect dead cells. C, ECCs expressing MEF2C or cardiac myosin increases with time. * $P < 0.05$, ** $P < 0.001$ versus 1 and 2 days.

stem cells.¹⁶ Importantly, the majority of CSCs in dogs,¹⁷ humans,⁷ and here in the mouse heart expresses together c-kit, MDR1, and Sca-1-like proteins. Additionally, these stem cell antigens are not associated with a significant difference in the ability of these primitive cells to acquire the myocyte, endothelial, and smooth muscle cell lineage in vitro¹⁷ and in vivo.^{7,17} The latter has been confirmed in the mouse heart. The ability of clonogenic c-kit^{POS} cells to create myocardial cells in vitro, however, is several-fold greater than cells expressing MDR1, Sca-1-like protein, or c-kit, MDR1, and Sca-1 together.¹⁷ Whether this in vitro property of c-kit^{POS} cells has a comparable in vivo counterpart remains an unanswered question.

The Infarcted Heart

Post-infarction cardiomyopathy is the major cause of heart failure, and the current observations offer new insights concerning the onset and evolution of this disease. On the basis of the present results, the progressive nature of ischemic cardiomyopathy appears to be dictated by the inability of CSCs-ECCs to translocate and home to the infarcted myocardium rather than by limitations in the growth reserve of the damaged heart. The resident stem cells distributed in the infarcted region do not survive the ischemic event and die by apoptosis and necrosis in a manner identical to that of myocytes and coronary vessels. CSCs-ECCs are not capable of opposing the death signals activated by permanent coronary occlusion and initiate regenerative growth within the infarcted myocardium. Moreover, these primitive cells cannot escape replicative senescence with severe telomeric shortening and activation of the death program in end-stage failure⁷ or premature myocardial aging¹⁹ in humans. Spontaneous myocardial regeneration within acute infarcts, however, appears to be mediated by CSCs-ECCs, which undergo lineage commitment and differentiation.⁷ With some exceptions,⁷ tissue growth does not invade and replace the infarcted myocardium but is restricted to the noninfarcted portion of the ventricular wall.²⁰ This is not a peculiar limitation

of the heart. Stem cells are efficient in maintaining organ homeostasis but do not prevent the formation of a scar after artery occlusion in the intestine, skin, brain, liver, kidney, and the bone marrow.^{21,22}

Consistent with previous observations of cardiac repair,^{1,5,17} early myocardial regeneration is characterized by the formation of immature parenchymal cells and coronary vessels that resemble the fetal heart. Cardiomyocytes, resistance arterioles, and capillary structures mature with time, but only $\approx 20\%$ of myocytes reach the adult phenotype and have a volume of 10 000 to 20 000 μm^3 4 months after successful treatment (Figure 6D). This is at variance with the process of postnatal development, as myocytes acquire adult characteristics at 3 to 4 weeks after birth. Interestingly, scattered regeneration of myocytes in the surviving myocardium after infarction results in the formation of parenchymal cells that are indistinguishable from the preexisting partners.⁵ This observation has led to the conclusion that contact with differentiated cells and paracrine factors may be implicated in the destiny of lineage-committed CSCs-ECCs.

On the basis of the belief that the heart lacks endogenous regenerative capacity, early strategies of cardiac repair have used the colonization of the myocardium with exogenous cells.²³ The presence of CSCs raises the unique prospect of reconstituting dead myocardium after infarction, repopulating the hypertrophic decompensated heart with new, better-functioning cells and vascular structures, and, perhaps, restoring the physiological and anatomical characteristics of the normal heart. These possibilities have formed the basis of a new paradigm in which the heart is viewed as a dynamic organ that constantly renews its cell populations and has the inherent ability to reconstitute tissue. Understanding cardiac homeostasis would offer the extraordinary opportunity to potentiate this naturally occurring process and promote myocardial repair after injury.²⁴

Rescue of the Infarcted Heart

So far, experimental studies and clinical trials have used rather heterogeneous bone marrow cell populations to regen-

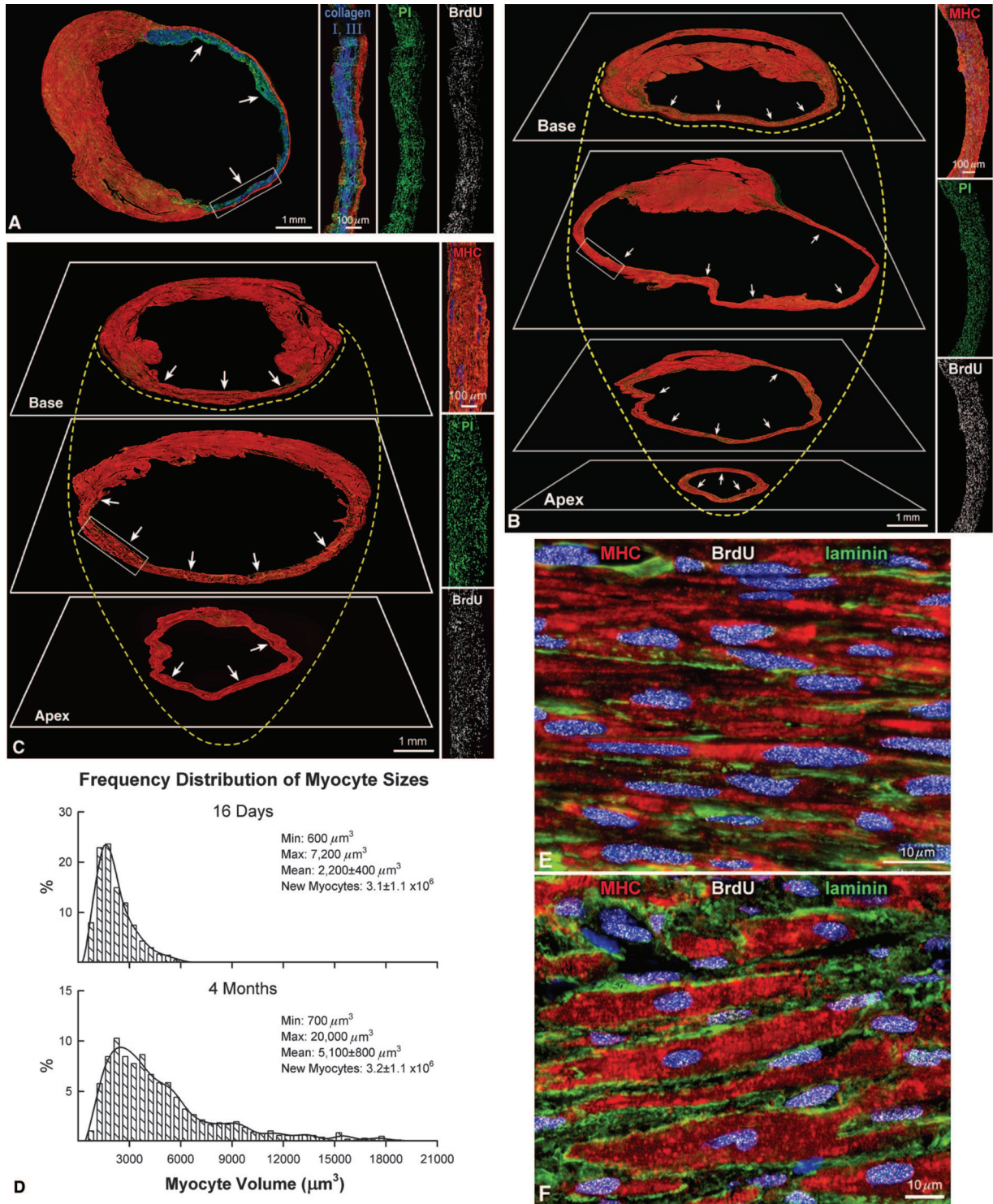


Figure 6. Myocardial regeneration. A through C, Untreated MI (A) and MI-Ts at 16 days (B) and 4 months (C). Arrows show infarcted nonregenerated (A) and infarcted regenerated (B and C) myocardium. BrdU^{POS} nuclei (A, fibroblasts). B and C, Four levels of regeneration from base to apex. Groups of 3 panels show areas within rectangles. Each triplet illustrates myocytes (cardiac myosin, red), collagen-type-I/type-III (blue), nuclei (PI, green), and BrdU^{POS} nuclei (white). BrdU labeling in regenerated-myocardium (B and C) indicates that cells were formed after infarction. D, Myocyte size distribution. E and F, New myocytes (cardiac-myosin, red) in GF-treated infarcted mice at 16 days (E) and 4 months (F). BrdU^{POS}-nuclei appear as white dots; laminin appears green.

erate infarcted myocardium and have consistently shown an improvement in function of the infarcted heart.²³ However, the most logical and potentially powerful cell to be used is the CSC. It is intuitively apparent that if the adult heart possesses

a pool of primitive multipotent cells, these cells have to be tested first before more complex and unknown cells are explored. The attraction of this approach is its simplicity. Cells from other organs are not programmed to give rise to

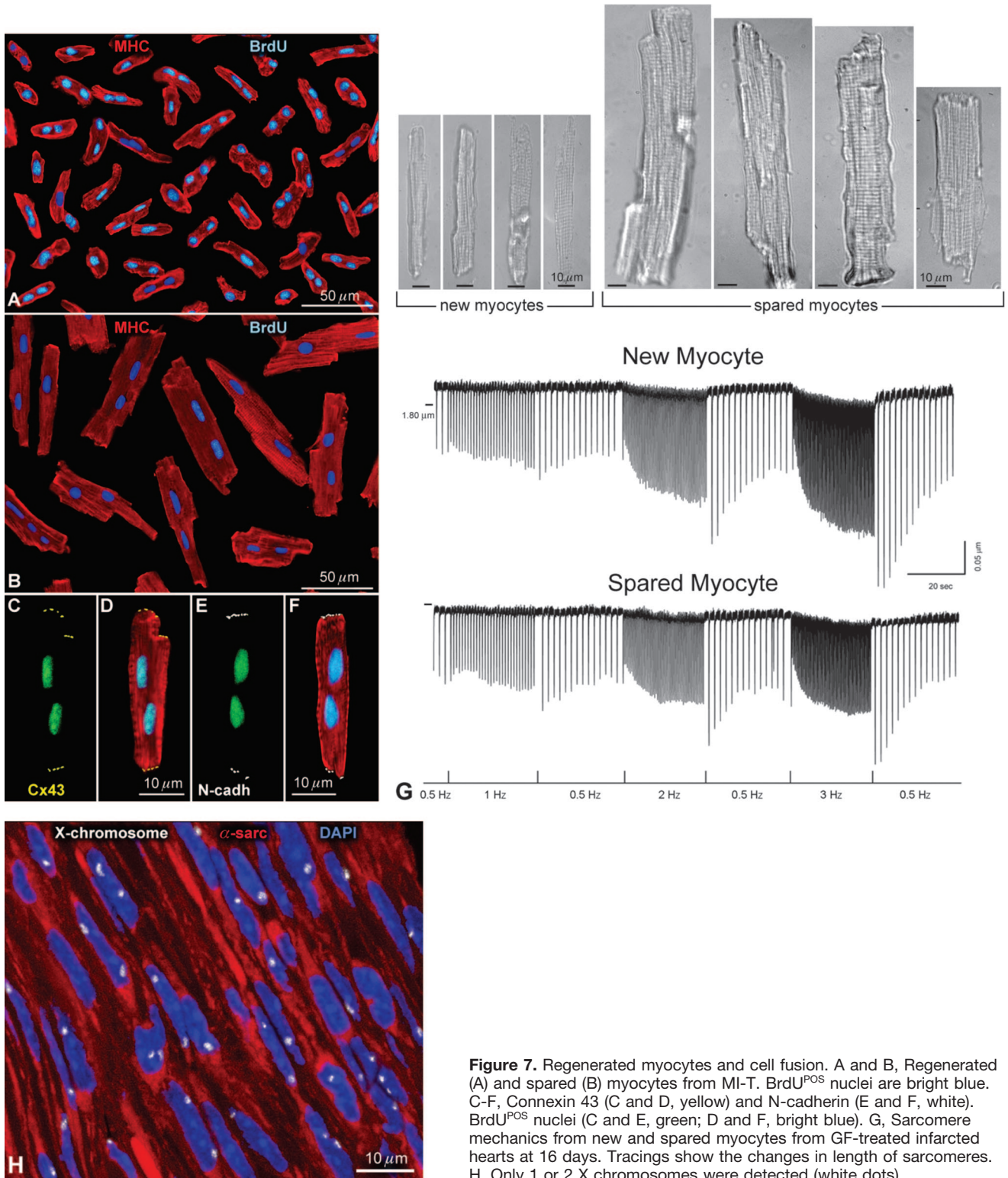


Figure 7. Regenerated myocytes and cell fusion. A and B, Regenerated (A) and spared (B) myocytes from MI-T. BrdU^{POS} nuclei are bright blue. C-F, Connexin 43 (C and D, yellow) and N-cadherin (E and F, white). BrdU^{POS} nuclei (C and E, green; D and F, bright blue). G, Sarcomere mechanics from new and spared myocytes from GF-treated infarcted hearts at 16 days. Tracings show the changes in length of sarcomeres. H, Only 1 or 2 X chromosomes were detected (white dots).

cardiomyocytes and coronary vessels, and transdifferentiation requires nuclear reprogramming with chromatin reorganization. This is a time-consuming process²⁵ that delays the formation of alternate progeny, affecting the onset and efficiency of myocardial regeneration. Conversely, the intramyocardial injection of GFs promotes the translocation of CSCs-ECCs to the damaged area and activates their growth

and differentiation, resulting in the formation of functionally competent myocardium. The blunted response to HGF or IGF-1 emphasizes the need for a dual stimulation of CSCs-ECCs: The survival and growth provided by IGF-1 together with the chemotactic effects of HGF. The presence of small new myocytes within the infarct at 1 to 2 days after coronary ligation demonstrates that tissue reconstitution is an immedi-

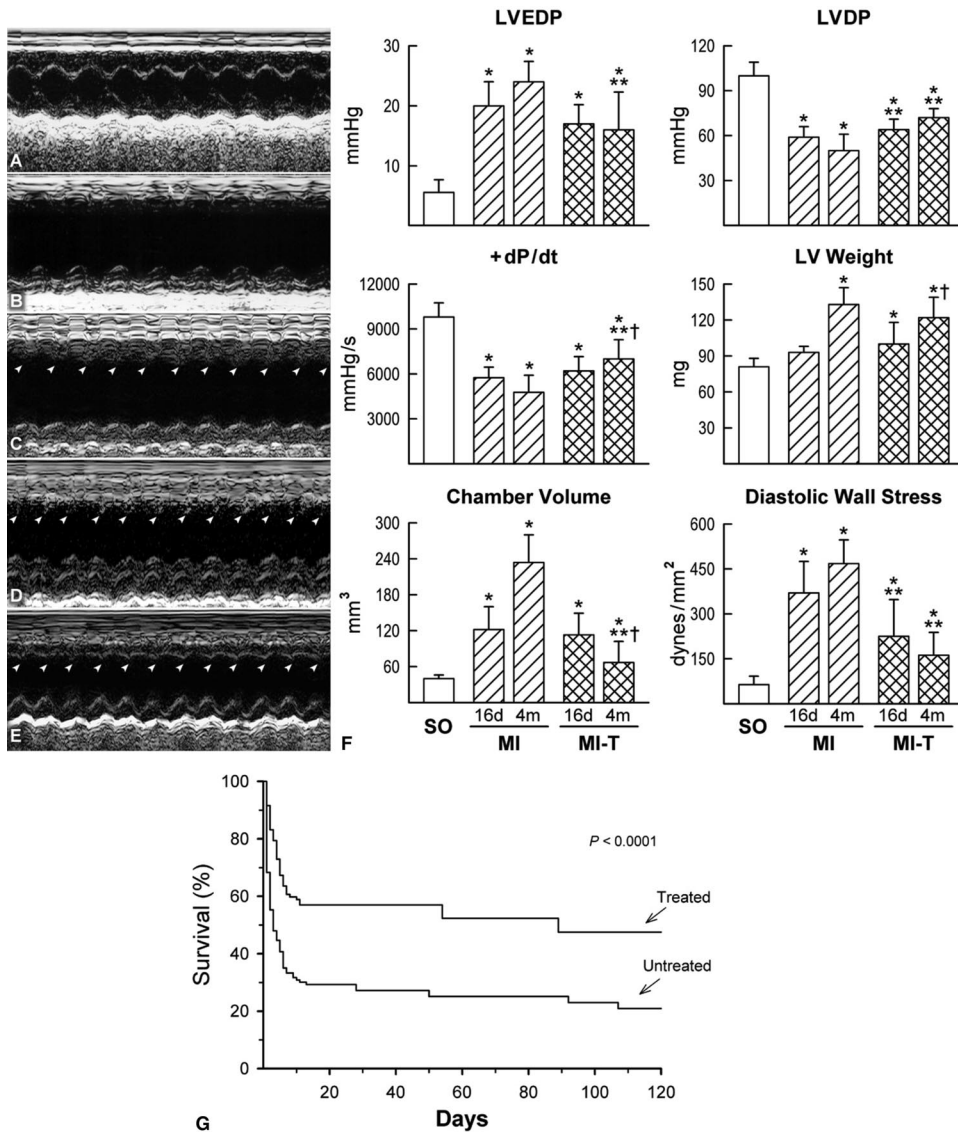


Figure 8. Cardiac function and mortality. A through E, Echocardiography of a noninfarcted-SO (A), untreated infarcted heart at 4 months (B), and GF-treated infarcted hearts at 15 days (C), 1 month (D), and 4 months (E). Contraction in the infarcted region is apparent in GF-treated mice at 15 days and thereafter (arrowheads). F, Functional properties of SO, untreated MI and MI-T. *, **, † $P < 0.05$ to 0.001 versus SO (*), MI (**), and MI-T at 16 days (†). G, Mortality after infarction was reduced in GF-treated mice ($P < 0.0001$; log-rank test) although these mice had $\approx 50\%$ larger infarcts.

ate reaction that restores an amount of myocardium larger than any other reported so far in the long term.

At variance with previous strategies,²³ local GF administration benefited animals with infarcts that are typically fatal. However, these results leave unanswered the question of why ischemia does not activate stem cells locally, favoring their homing to the damaged area, or whether the effects of GFs on ischemic myocytes influenced cell viability. Myocardial ischemia is a potent inducer of IGF-1²⁶ and HGF.²⁷ The injection of GFs did not increase the number of bone marrow progenitor cells in the circulation, as shown by the lack of changes in the pool of CD45 and c-kit^{POS} cells in the peripheral blood (supplemental Figure S29); 240 μg of HGF over a period of 12 days was required to produce a modest increase in circulating BMPCs.²⁸ This quantity is 170 000-fold higher than the 1.4 ng given here at a single time point (limitations; online).

Cell Migration

The locomotion of CSCs-ECCs occurs through the myocardial interstitium independently from the coronary circulation. CSCs-ECCs traverse in vitro a 3-dimensional substrate of

Matrigel and in vivo dense barriers of collagen type I and III. MMP-2 and MMP-9 appear to be the proteolytic enzymes responsible for the invasive phenotype of CSCs-ECCs and their trafficking across the myocardial interstitium. However, MMP-9 may trigger the release of stem cell factor²⁹ from CSCs-ECCs, although stem cell factor has no effects on the invasive properties of these cells in vitro.¹⁷

The migratory elements of CSCs-ECCs may include motogenic factors, and ischemia is a potent inducer of the chemoattractants HGF, stromal cell-derived factor-1, and vascular endothelial growth factor. Although these cytokines may favor cell movement, it is only with HGF that waves of CSCs-ECCs are engaged in a directional migration toward the injured myocardium. A stop signal may also be present to promote the accumulation of cells within the infarct. This involves the extracellular substrates used by the cells to traverse the interstitium. The ability of CSCs-ECCs to degrade extracellular matrix provides a basis for the tunnel tracks found in the myocardium. CSCs-ECCs adhere to the wall of fibronectin that delimit the interstitial channels. Importantly, fibronectin is implicated in the migration of c-kit^{POS} cells.³⁰ Finally, the directional locomotion

of cells is regulated by guidance factors. Ligand-receptor systems are potential candidates for defining the trajectory of migrating CSCs-ECCs and, in our conditions, the activation of c-Met by HGF may be the determinant element. MMPs, together with the HGF-mediated changes in integrin phenotype of CSCs-ECCs (A.L., unpublished data), may be crucial for effective translocation of cells. Other systems, including the c-Met-related family of semaphorins and neuropilins, are likely to be involved. The long journey of a stem cell toward its final destination, however, remains an intriguing and mysterious event.

Acknowledgments

This work was supported by National Institutes of Health grants HL-38132, AG-15756, HL-65577, HL-66923, HL-65573, AG-17042, AG-023071, AG-026107, HL-43023, HL-50142, and HL-081737.

References

- Beltrami AP, Barlucchi L, Torella D, Baker M, Limana F, Chimenti S, Kasahara H, Rota M, Musso E, Urbanek K, Leri A, Kajstura J, Nadal-Ginard B, Anversa P. Adult cardiac stem cells are multipotent and support myocardial regeneration. *Cell*. 2003;114:763–776.
- Oh H, Bradfute SB, Gallardo TD, Nakamura T, Gausson V, Mishina Y, Pocius J, Michael LH, Behringer RR, Garry DJ, Entman ML, Schneider MD. Cardiac progenitor cells from adult myocardium: homing, differentiation, and fusion after infarction. *Proc Natl Acad Sci U S A*. 2003;100:12313–12318.
- Matsuura K, Nagai T, Nishigaki N, Oyama T, Nishi J, Wada H, Sano M, Toko H, Akazawa H, Sato T, Nakaya H, Kasunuki H, Komoro I. Adult cardiac Sca-1-positive cells differentiate into beating cardiomyocytes. *J Biol Chem*. 2004;279:11384–11391.
- Pfister O, Mouquet F, Jain M, Summer R, Helmes M, Fine A, Colucci WS, Liao R. CD31- but not CD31+ cardiac side population cells exhibit functional cardiomyogenic differentiation. *Circ Res*. 2005;97:52–61.
- Dawn B, Stein AB, Urbanek K, Rota M, Whang B, Rastaldo R, Torella D, Tang XL, Rezazadeh A, Kajstura J, Leri A, Hunt G, Varma J, Prabhu SD, Anversa P, Bolli R. Cardiac stem cells delivered intravascularly traverse the vessel barrier, regenerate infarcted myocardium, and improve cardiac function. *Proc Natl Acad Sci U S A*. 2005;102:3766–3771.
- Messina E, De Angelis L, Frati G, Morrone S, Chimenti S, Fiordaliso F, Salio M, Battaglia M, Latronico MV, Coletta M, Vivarelli E, Frati L, Cossu G, Giacomello A. Isolation and expansion of adult cardiac stem cells from human and murine heart. *Circ Res*. 2004;95:911–921.
- Urbanek K, Torella D, Sheikh F, De Angelis A, Nurzynska D, Silvestri F, Beltrami CA, Bussani R, Beltrami AP, Quaini F, Bolli R, Leri A, Kajstura J, Anversa P. Myocardial regeneration by activation of multipotent cardiac stem cells in ischemic heart failure. *Proc Natl Acad Sci U S A*. 2005;102:8692–8697.
- Powell EM, Mars WM, Levitt P. Hepatocyte growth factor/scatter factor is a motogen for interneurons migrating from the ventral to dorsal telencephalon. *Neuron*. 2001;30:79–89.
- Hamasuna R, Kataoka H, Moriyama T, Itoh H, Sekki M, Koono M. Regulation of matrix metalloproteinase-2 (MMP-2) by hepatocyte growth factor/scatter factor (HGF/SF) in human glioma cells: HGF/SF enhances MMP-2 expression and activation, accompanying up-regulation of membrane type 1 MMP. *Int J Cancer*. 1999;82:274–281.
- Rappolee DA, Iyer A, Patel Y. Hepatocyte growth factor and its receptor are expressed in cardiac myocytes during early cardiogenesis. *Circ Res*. 1996;78:1028–1036.
- Birchmeier C, Brohmann H. Genes that control the development of migrating muscle precursor cells. *Curr Opin Cell Biol*. 2000;12:725–730.
- Arsenijevic Y, Weiss S, Schneider B, Aebischer P. IGF-1 is necessary for neural stem cell proliferation and demonstrates distinct actions of epidermal growth factor and fibroblast growth factor-2. *J Neurosci*. 2001;21:7194–7202.
- Li Q, Li B, Wang X, Leri A, Jana KP, Liu Y, Kajstura J, Baserga R, Anversa P. Overexpression of insulin-like growth factor-1 in mice protects from myocyte death after infarction, attenuating ventricular dilation, wall stress, and cardiac hypertrophy. *J Clin Invest*. 1997;100:1991–1999.
- Rudnicki MA. Marrow to muscle, fission versus fusion. *Nat Med*. 2003;9:1461–1462.
- Martin CM, Meeson AP, Robertson SM, Hawke TJ, Richardson JA, Bates S, Goetsch SC, Gallardo TD, Garry DJ. Persistent expression of the ATP-binding cassette transporter, Abcg2, identifies cardiac SP cells in the developing and adult heart. *Dev Biol*. 2004;265:262–275.
- Laugwitz KL, Moretti A, Lam J, Gruber P, Chen Y, Woodard S, Lin LZ, Cai CL, Lu MM, Reth M, Platoshyn O, Yuan JX, Evans S, Chien KR. Postnatal isl1+ cardioblasts enter fully differentiated cardiomyocyte lineages. *Nature*. 2005;433:647–653.
- Linke A, Muller P, Nurzynska D, Casarsa C, Torella D, Nascimbene A, Castaldo C, Cascapera S, Bohm M, Quaini F, Urbanek K, Leri A, Hintze TH, Kajstura J, Anversa P. Stem cells in the dog heart are self-renewing, clonogenic and multipotent and regenerate infarcted myocardium, improving cardiac function. *Proc Natl Acad Sci U S A*. 2005;102:8966–8971.
- Urbanek K, Quaini F, Tasca G, Torella D, Castaldo C, Nadal-Ginard B, Kajstura J, Quaini E, Anversa P. Intense myocyte formation from cardiac stem cells in human cardiac hypertrophy. *Proc Natl Acad Sci U S A*. 2003;100:10440–10445.
- Chimenti C, Kajstura J, Torella D, Urbanek K, Heleniak H, Colucci C, Di Meglio F, Nadal-Ginard B, Frustaci A, Leri A, Maseri A, Anversa P. Senescence and death of primitive cells and myocytes lead to premature cardiac aging and heart failure. *Circ Res*. 2003;93:604–613.
- Beltrami AP, Urbanek K, Kajstura J, Yan SM, Finato N, Bussani R, Nadal-Ginard B, Silvestri F, Leri A, Beltrami CA, Anversa P. Evidence that human cardiac myocytes divide after myocardial infarction. *N Engl J Med*. 2001;344:1750–1757.
- Hudson DA, Goddard EA, Millar KN. The management of skin infarction after meningococcal septicaemia in children. *Br J Plast Surg*. 1993;46:243–246.
- Iuliano L, Gurgo A, Gualdi G, Bonavita MS. Succeeding onset of hepatic, splenic, and renal infarction in polyarteritis nodosa. *Am J Gastroenterol*. 2000;95:1837–1838.
- Wollert KC, Drexler H. Clinical applications of stem cells for the heart. *Circ Res*. 2005;96:151–163.
- Leri A, Kajstura J, Anversa P. Cardiac stem cells and mechanisms of myocardial regeneration. *Physiol Rev*. In press.
- Pomerantz J, Blau HM. Nuclear reprogramming: a key to stem cell function in regenerative medicine. *Nat Cell Biol*. 2004;6:810–816.
- Cheng W, Reiss K, Li P, Chun MJ, Kajstura J, Olivetti G, Anversa P. Aging does not affect the activation of the myocyte insulin-like growth factor-1 autocrine system after infarction and ventricular failure in Fischer 344 rats. *Circ Res*. 1996;78:536–546.
- Ueda H, Nakamura T, Matsumoto K, Sawa Y, Matsuda H, Nakamura T. A potential cardioprotective role of hepatocyte growth factor in myocardial infarction in rats. *Cardiovasc Res*. 2001;51:41–50.
- Yu CZ, Hisha H, Li Y, Lian Z, Nishino T, Toki J, Adachi Y, Inaba M, Fan TX, Jin T, Iguchi T, Sogo S, Hosaka N, Song TH, Xing J, Ikehara S. Stimulatory effects of hepatocyte growth factor on hemopoiesis of SCF/c-kit system deficient mice. *Stem Cells*. 1998;16:66–77.
- Heissig B, Hattori K, Dias S, Friedrich M, Ferris B, Hackett NR, Crystal RG, Besmer P, Lyden D, Moore MA, Werb Z, Rafii S. Recruitment of stem and progenitor cells from the bone marrow niche requires MMP-9 mediated release of kit-ligand. *Cell*. 2002;109:625–637.
- Takano N, Kawakami T, Kawa Y, Asano M, Watabe H, Ito M, Soma Y, Kubota Y, Mizoguchi M. Fibronectin combined with stem cell factor plays an important role in melanocyte proliferation, differentiation and migration in cultured mouse neural crest cells. *Pigment Cell Res*. 2002;15:192–200.